

Membrane Modification with Nanofiber Structures Containing Silver

Jan Dolina,* Tomáš Jiříček, and Tomáš Lederer

Centre for Nanomaterials, Advanced Technologies and Innovation, Technical University of Liberec, Studentská 1402/2, 461 17 Liberec 1, Czech Republic

ABSTRACT: Commercial ultrafiltration membranes were modified using different polymeric nanofibers in order to gain additional water treatment functionality. Membrane surfaces were given biocidal properties by adding electrospun nanofiber structures containing various forms of silver. Changes in viscosity and homogeneity of the electrospinning solution caused by the additives limited the amount of silver that could be added; hence, electrospinning conditions were optimized to maximize silver particle content. Best results were obtained using highly soluble silver nitrate and silver benzoate as silver nanoparticle precursors. The biocidal properties of the modified membranes were confirmed through cultivation techniques and respirometry, with the results indicating that ultrafiltration membranes modification using silver-treated nanofibers is a promising technique.

1. INTRODUCTION

Recent scientific research on ultrafiltration (UF) membranes has concentrated on modifications to improve filtration characteristics at the nanolevel. The pores in an ideal membrane should remain unblocked throughout the filtration process; pore blocking, however, frequently occurs, because of the passage of both inorganic and organic compounds, including metabolism byproducts of microorganisms.¹ Therefore, the prevention of microbial growth on a membrane's surface is essential in order to avoid frequent chemical and mechanical membrane cleaning.

Three different UF membrane nanomodification concepts can be distinguished:

- Dispersion of inorganic nanoparticles directly into the membrane structure.²
- Incorporation of active catalytic compounds in polyelectrolyte, in combination with layer-by-layer polyelectrolyte surface modification of the membrane.³
- The use of nanofibers for membrane construction, with membrane modification through incorporation of nanoparticles.

In this study, we focus on nanofibers with incorporated silver nanoparticles⁴ and integration of such nanofiber layers into membrane topcoats in order to increase antibacterial properties. This type of modified membrane is proposed for the filtration of organically contaminated water and for possible use in membrane bioreactors.

2. MATERIALS AND METHODS

2.1. Materials. Polymeric Nanofibers. Nanofibers were prepared by electrospinning,⁵ whereby fibers are formed from a thin layer of polymer solution through the effects of an electrostatic field (Figure 1). The capability of a polymer to form fibers is affected by several process and system parameters, such as the intensity of electric field, viscosity, molar mass, surface tension, and polymer concentration. Two types of polymeric nanofiber layer were used in these experiments: polyurethane (PU), which is the most abrasion-resistant elastomeric polymer, displaying mechanical stability, good

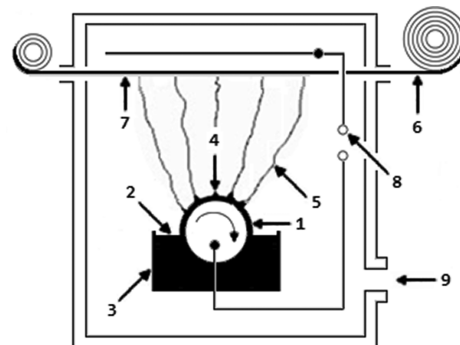


Figure 1. Illustration of the free surface electrospinning equipment used.⁸ Legend: (1) metal roller, (2) polymer solution, (3) solution reservoir, (4) Taylor cone, (5) fiber casting direction, (6) support material, (7) nanofiber sheet, (8) ground electrode, and (9) air conditioning.

chemical resistance, and long-term heat resistance. Its hydrolytic stability surpasses that of polymeric amides.⁶ Furthermore, PU nanofibers have known hydromechanical properties and a proven ability to be electrospun.⁵ The second nanofiber type, polyethersulfone (PES), is a transparent, heat-resistant, high-performance engineering thermoplastic with excellent dimensional stability and chemical resistance. Both polymers exhibit low water solubility.

The PU used for nanofiber production was based on a 30% standard solution (Larithane) in dimethylformamide (DMF; Penta; ≥ 99.5%) provided by Novotex. Dimethylacetamide (DMAc; Aldrich; ≥ 99.5%), dimethylsulfoxide (DMSO; Penta; > 99%), and *N*-methyl-2-pyrrolidone (NMP; Aldrich; ≥ 99%) were used as alternatives to DMF in experiments, while tetraethylammonium bromide (TEAB, Aldrich, > 98%) was

Special Issue: Recent Advances in Nanotechnology-based Water Purification Methods

Received: November 13, 2012

Revised: February 27, 2013

Accepted: March 1, 2013

Published: March 1, 2013

added to obtain the necessary conductivity for experimental silver-free nanofibers.

PES nanofibers were prepared from BASF E 6020P polymer. A range of solvents⁷ were tested (based on Hansen solubility parameters), and these produced different fiber results. The solvents used for finding appropriate functional samples, in terms of electrospinning and nanofiber properties, were DMF, NMP, *N*-ethyl-2-pyrrolidone (NEP; Aldrich; >98%), DMSO, DMAc, and additives. All chemicals were used without further purification.

Silver Addition. Three different silver precursors were tested: silver nitrate (AgNO_3 ; Penta; ≥99.8%), silver benzoate ($\text{C}_7\text{H}_5\text{AgO}_2$; Aldrich; ≥99%), and silver behenate ($\text{C}_{22}\text{H}_{43}\text{AgO}_2$; TCI; >95%). In addition, two types of silver dispersion were tested: water dispersion of zerovalent silver (3000 mg/L) with polyacrylate surface stabilizer (Palacky University Olomouc), and organic dispersion of 5% silver behenate in NEP (Agfa).

2.2. Methods. Preparation of Nanofiber Solutions. The PU standard solution, silver solution, and solvent or reducing agent were mixed together; then, a solvent was added in order to obtain a polymer concentration (typically 14%–18%) and viscosity suitable for nanofiber electrospinning.

For preparation of the PES polymer, the solid polymeric phase and the solvent-reducing silver system were mixed; then, a solvent was added to obtain the appropriate electrospinning polymer concentration (typically 15%–20%). These solutions were then stirred overnight. Immediately before electrospinning, the samples were placed into an ultrasound bath and heated to 65 °C for ~15 min to increase polymer chain mobility.

Nanofiber Casting Method. The free surface electrospinning method⁸ was used for both laboratory-prepared and continuously prepared nanofibers (Figure 1). Small-scale laboratory samples were prepared using an aluminum rod as the positive electrode and a magnetic steel plate as the ground electrode. The viscous nanofiber solution was placed between the electrodes, and the fibers cast onto black office paper (80 g/m²). The electrostatic field was generated using a Spellman SL70PN150 power supply with a voltage range of 25–35 kV (maximum 70 kV) and an electrode distance of 10–12 cm. The experiment took place in a fume cupboard with air conditioning and a KRÜGER 370W Airsec 125 dehumidifier for regulation of relative humidity (RH).

Large-scale samples were produced by continuous electrospinning (Figure 1). The nanofiber solution was placed in a reservoir with a positively charged drum. We used a Spelmann SL 600W high-voltage source with a voltage range of 60–75 kV (maximum of 120 kV), with a round roller and spiked roller used for electric field intensification for PU and PES nanofibers, respectively; the electrode distance being set between 15 and 17 cm. RH was regulated by heated air conditioning. The solution was cast onto spunbond PP (Pegas; nonwoven) with a winding speed of 0.05–0.1 m/min.

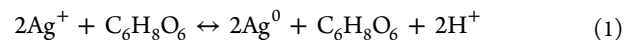
Morphological Analysis and Particle Size Distribution. Morphological analysis was undertaken using the FEI Phenom scanning electron microscopy (SEM) system in the Department of Nonwoven Textiles of the Technical University in Liberec (TUL), and a JEOL Model JSM-6340F microscope, with the cooperation of the Flemish Institute for Technological Research (VITO). The nanofibers were scanned either uncoated, or coated with a 2.5-nm layer of platinum (Pt)/palladium (Pd) (80/20), and images obtained at an

acceleration voltage of 20 kV and 5 kV, respectively. The FEI Tecnai microscope was used for transmission electron microscopy (TEM) analysis, with the cooperation of Institute of Macromolecular Chemistry of the Academy of Sciences of the Czech Republic.

Monodisperse particle size distribution was measured using a light scattering Malvern ZetaSizer instrument, which allowed us to confirm the initial reported silver particle size within the aqueous dispersion⁹ (i.e., 15 nm). Measurement of polydisperse particles in the nanofiber was affected by high variation in particle size distribution and time dependency caused by particle sedimentation. In order to avoid inconsistency, therefore, we measured particle size distribution using NIS-Elements AR 3.10 (Nikon) image analysis.

Silver Nanoparticle Reduction Methods. Compared to ionic silver, zerovalent silver shows lower cytotoxicity, increased antibacterial activity, and lower coagulation in environments with high ionic strength.⁹

Many different solvent reduction methods were tested, including reduction in DMF,¹⁰ ex-post-reduction methods using ascorbic acid¹¹ (eq 1) and ultraviolet irradiation.¹² For ascorbic acid reduction, we used its 3% solution in demineralized (DEMI) water and applied it directly on the nanofiber surface by spraying.



In order to reduce the chemical influence and avoid undesirable morphological changes to the nanofibers, application of long-wave UVA light (315–400 nm), using a Philips TUV 25W lamp, was also investigated.

Preparation of Composite Membranes. Several nanofiber layer thermal pressure fixation experiments were performed on flat-sheet Microdyn-Nadir UP150 PES UF membranes¹³ (150 kDa; polypropylene (PP)/polyethylene terphthalate substrate). Lamination tests were undertaken using an OSHIMA OP-450GS Mini Press (temperature, 0–230 °C; maximum pressure, 0.14 MPa), with Teflon surface coating on the molding strip. Continuously electrospun nanofiber layers were thermally detached from the support layer and laminated onto the membrane's surface in order to complete the membrane composite.

Nanofiber Deposition Directly onto the Membrane Surface. In order to avoid membrane degradation caused by lamination, we also examined direct fiber deposition onto the membrane's surface by electrospinning. Nanofibers prepared under the correct electrospinning conditions¹⁴ are able to show excellent adhesion to the test surface. Direct deposition was undertaken by attaching a membrane to the PP nonwoven substrate and casting nanofibers by continuous electrospinning.

Membrane Testing. Membrane Permeability. Permeability measurements were undertaken using a 50-mL Millipore/Amicon 8050 dead-end cell driven by nitrogen pressure and an Alfa Laval M10 cross-flow unit, operated under constant-volume operational mode and using DEMI water at room temperature as the filtration liquid.

Leaching of Silver from the Nanofiber Layer. Two modes of silver stability were tested: (a) silver concentration in permeate measured through filtration of 50 mL of DEMI water through dead-end and cross-flow units and (b) based on leaching from dry samples measured by agitating the modified membrane in DEMI water. An exact volume was taken at regular intervals for inductively coupled plasma optical emission spectrometry (ICP-OES) analysis, i.e., 0, 5, 15, 30, 60, and 120

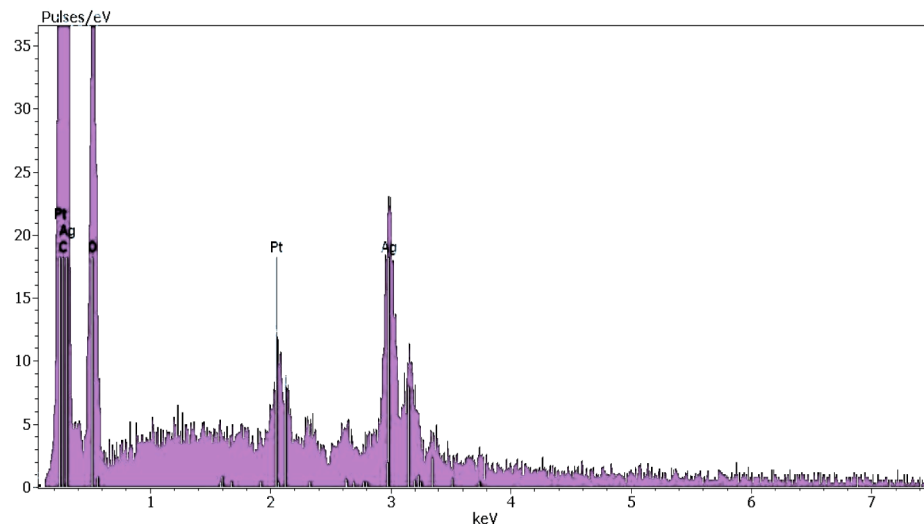


Figure 2. Results of X-ray diffraction (XRD) analysis for polyurethane nanofibers containing silver.

min for short tests; and 0, 1 h, 1 day, and 4 days for medium-term tests. Integrated sampling involved one volume per each membrane and samples were taken from the continuously concentrating liquid. For the derivation method, the same membrane was placed in a new volume of DEMI water following each sample and the respective silver concentrations added together. For both methods, the resulting total silver content should be identical.

Nitric acid was added to each sample volume to obtain a 1% acidic solution and the sample was then analyzed on an ICP Optima 2100 DV spectrometer with argon as the inert phase and calibration set by three points 0, 1, and 10 mg/L standard curve.

To determine the total amount of silver, the nanofiber structure was separated from the carrier and, following mineralization, the samples were converted to a 50-mL volume and the absolute concentration calculated.

Antimicrobial Testing. The antibacterial properties of the composite membranes were tested by (a) filtering a *Escherichia coli* (reference number according to ČSNI: CCM 3954) bacterial solution through the membrane in a dead-end and cross-flow arrangement, then cultivating the bacteria on the membrane's surface and observing growth; and (b) using an online respiration activity monitoring system. Oxygen transfer rate was found to be the most suitable parameter for quantifying the physiological state of the aerobic microorganism culture as most metabolic activities depended on oxygen consumption.¹⁵ These measurements were undertaken in cooperation with the NAMETECH project partner, RWTH Aachen University.

For midterm leached membranes, we use this biocide test: *E. coli* bacteria (CCM 3954) were inoculated onto growing Plate Count Agar substrate. After significant growth, bacterial forming units were dispersed into saline and the absorbance measured at 600 nm (OD 600) on a Hach-Lange DR2800 laboratory analysis spectrophotometer. This wavelength corresponds to the inner phase of *E. coli* growth. For cell calculation, we use a linear relation¹⁶ that a saturated *E. coli* culture has $\sim 1 \times 10^9$ cells/mL.

In our case, an absorbance value of 0.712 represented 7.12×10^8 cell/mL. We diluted the initial solution 1:700 to get $\sim 1 \times 10^5$ cells/mL (sample A), and 1:70 to obtain a concentration of

1×10^6 cells/mL (sample B). A 10 mL sample of A was then added to two 2 cm \times 2 cm silver-coated membranes, and 10 mL of B into a third sample. The membranes were previously leached for 4 days, and then they were intensively washed with demineralized water to ensure that no previously leached silver remained attached to the membrane's surface. During the *E. coli* tests, we considered that reaction of silver with Cl⁻ ions from the saline as negligible. We used two blank samples of saline for comparison.

The *E. coli* samples were incubated for 24 h at 37 °C, while the samples were stirred by hand at 0, 12, and 24 h. Subsequently, 1 mL of 0, -1, -2, -3, and -4 log diluted samples were placed on Agar plates filled with Plate Count Agar medium without dextrose. The samples were then kept under aerobic conditions for 48 h at 37 °C for cultivation.

3. RESULTS AND DISCUSSION

3.1. PU Nanofibers. The addition of silver particles to the spinning solution negatively affected both homogeneity and

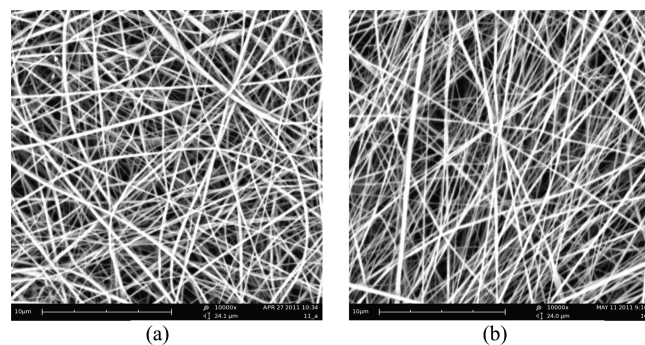


Figure 3. Differing morphology of polyethersulfone (PES) nanofiber samples: (a) 15% in DMFO/DMS, fiber diameter = 205 ± 67 nm and (b) 20% in DMF/NMP, fiber diameter = 174 ± 51 nm. Images obtained using the FEI scanning electron microscopy (SEM) system (accelerating voltage = 20 kV; magnification = 10 000 \times).

fiber structure, resulting in a wider fiber diameter, compared to pure PU nanofibers. The surface charge of silver particles had a major impact by limiting the mobility of the charged polymer group when the electric field was applied.

Table 1. Polyethersulfone (PES) and Polyurethane (PU) Nanofibers Produced in the Laboratory Using Different Types of Silver^a

silver type	form	PU		PES	
		content [wt _{Ag} /wt _p]	particle diameter [nm]	content [wt _{Ag} /wt _p]	particle diameter [nm]
Ag(0) particles	dispersion	0.003	300 ± 120 ^b		
silver behenate	dispersion	0.008	150 ± 59	0.012	100 ± 42
silver nitrate	salt	0.220	80 ± 21	0.140	90 ± 35
silver benzoate	salt	0.100	60 ± 28	0.080	40 ± 24
silver behenate	salt	0.005	230 ± 76	0.008	200 ± 79

^aThe mean fiber diameter (180–300 nm) depended on the process conditions and particle morphology. ^bMeasurement made using a light scattering device.

Table 2. Polyethersulfone (PES) and Polyurethane (PU) Nanofibers Prepared by Continuous Electrospinning

silver type	PU		PES	
	silver nitrate	silver benzoate	silver benzoate	silver behenate
concentration [wt _p /wt _{Ag}]	0.22	0.07	0.04	0.01
fiber diameter [nm]	240 ± 64	180 ± 75	190 ± 47	290 ± 114
solvent type	DMF	DMF/DMAc	DMF/DMAc	DMF/NMP/DMSO ^a
content [%]	100	50/50	50/50	47/41/12

^aDMSO was added for higher solution conductivity.

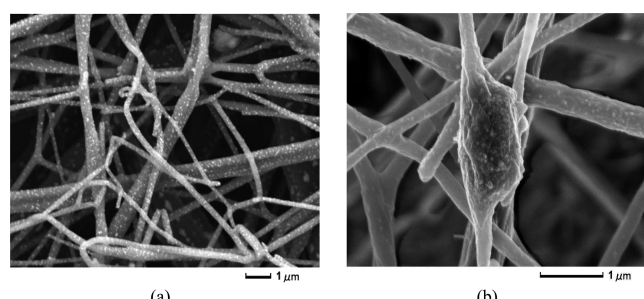


Figure 4. Continuously prepared polyurethane (PU) nanofibers with silver nitrate. Images were obtained using the JEOL-JSM microscope at VITO (accelerating voltage = 5 kV); magnification = (a) 10 000× and (b) 25 000×.

Under laboratory conditions, we observed a plasma effect, i.e., a flow of ions and partially charged molecules that formed a blue/red (violet) light (forming a crown) on droplet boundaries when the solution was not spinning readily. This plasma flow was possibly caused by a loss of silver valence electrons in the strong electric field or by ionization of air molecules.

In tests based on the dispersion of silver in water, we observed both low silver concentration (~0.3 wt %) and high mean aggregate size (300 nm). Silver nitrate appeared to suppress negative phenomena in the electrospinning process, having a positive impact on both structure and distribution of particles in the final sample. The concentration of silver in PU nanofibers was ~22% of polymer weight (wt_p), with the specific concentration of silver reaching 800–1200 mg/m² for nanofiber sheets prepared using continuous electrospinning and cast onto PP supports. At a winding speed of 0.05 cm/min, the weight of the nanofiber layer, following separation from the support, was 6.5–7.2 g/m².

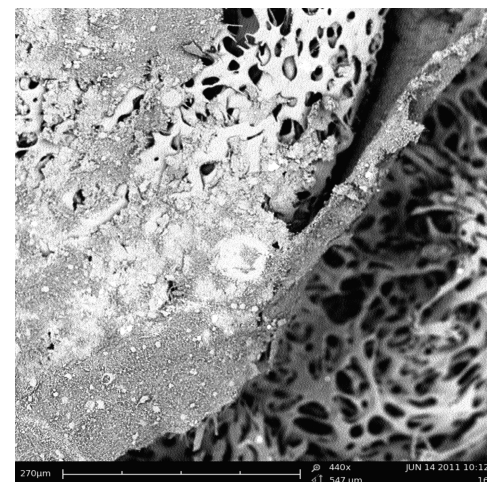


Figure 5. Image of a polyethersulfone (PES) ultrafiltration membrane with nanofiber layer. Image obtained on the FEI scanning electron microscope (accelerating voltage = 20 kV; magnification = 440×).

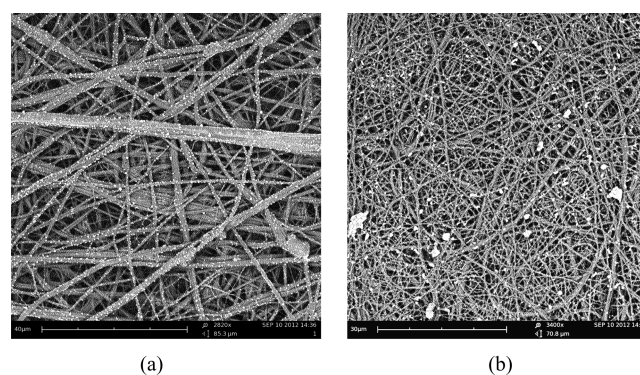


Figure 6. Scanning electron microscopy (SEM) images of dry samples after (a) 1 min and (b) after 10 min in DEMI water (accelerating voltage = 20 kV).

Both conductivity measurements and ICP-OES analysis of the cast solution before and after electrospinning indicated that silver particles were not cast preferentially. The ICP-OES measurements also indicated that the ratio of silver before and after spinning was almost the same (0.95). Despite high dilution rates (1000× and 2000×); therefore, we were able to achieve comparable results. Silver presence was secondarily confirmed using X-ray diffraction (XRD) particle spectra (Department of Chemistry, TUL) (see Figure 2).

Mean particle size for silver nitrate was ~80 nm. Dilute silver solutions ensured easier electrospinning as the required

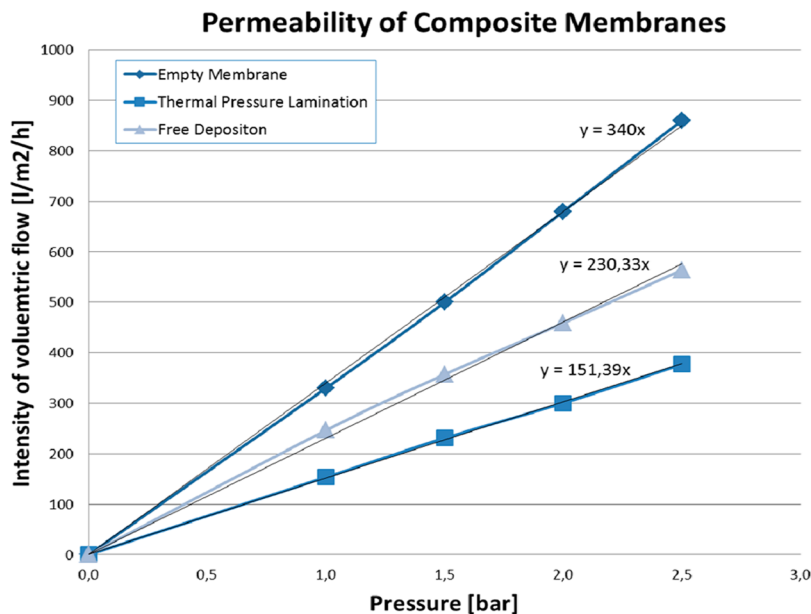


Figure 7. Improved permeability achieved by direct deposition on a membrane's surface.

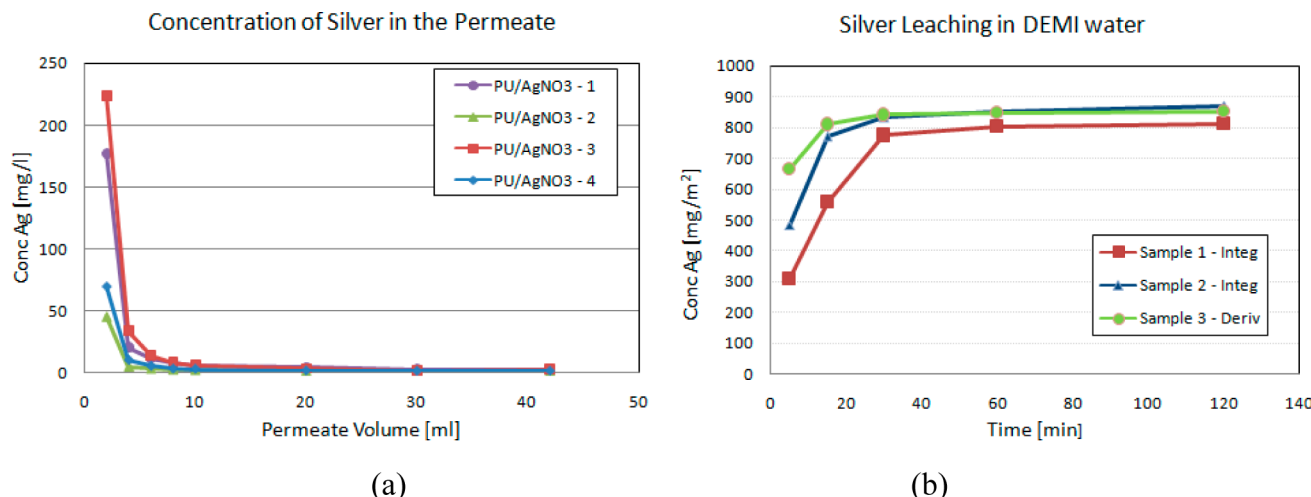


Figure 8. (a) Leaching characteristics of silver at different initial concentrations, and (b) silver leaching in DEMI water.

Table 3. *E. coli* Bacteria Count after 48 h Cultivation for 0 to -4 Log Dilution^a

log dilution	Bacteria Count (CFU/mL)				
	1	2	3	4	5
0	2	2	2	364	247
-1	1	0	0	38	26
-2	0	0	0	4	2
-3	0	0	0	0	0
-4	0	0	0	0	0

^aSamples 1–3 are the silver-leached membranes. The initial *E. coli* cell concentration of sample 3 was 10 times higher than that of samples 1 and 2. Samples 4 and 5 are blank samples

conductivity could be maintained longer; however, it also resulted in lower concentrations and uneven particle distribution. Higher silver concentrations (typically >15% of silver, relative to polymer weight), depending on the solvent system used, tended to suppress electrospinning efficiency. The optimal silver concentration lies between these extremes.

Using the silver behenate precursor (DMF/DMSO solvent system), the particle size was ~230 nm and the delivery was nonhomogeneous. Similarly, the electrospun NEP/silver behenate dispersal solution displayed low homogeneity and low density. The use of silver behenate as an additive, therefore, is limited by its low solubility. On the other hand, low solubility should result in prolonged release of silver.

Mean particle size for the silver benzoate solution (DMF/DMSO) was ~60 nm (10% wt_p), with a minimum particle size in the range of 20 nm, the resolution of the SEM being the limiting factor for detection (18 nm at the 12000 \times range). Silver benzoate is formed from longer chains with different mobility than silver nitrate and, therefore, has a lower tendency to reaggregate in a strong electric field.

For effective antibacterial activity, it is important that silver activity takes place directly on the surface of the nanofiber. Large silver particles cannot be transported to the nanofiber's surface; small particles at the nanometer scale, however, can and show more effective antibacterial activity, because of diffusion transport.¹⁷ The preliminary results of TEM imaging

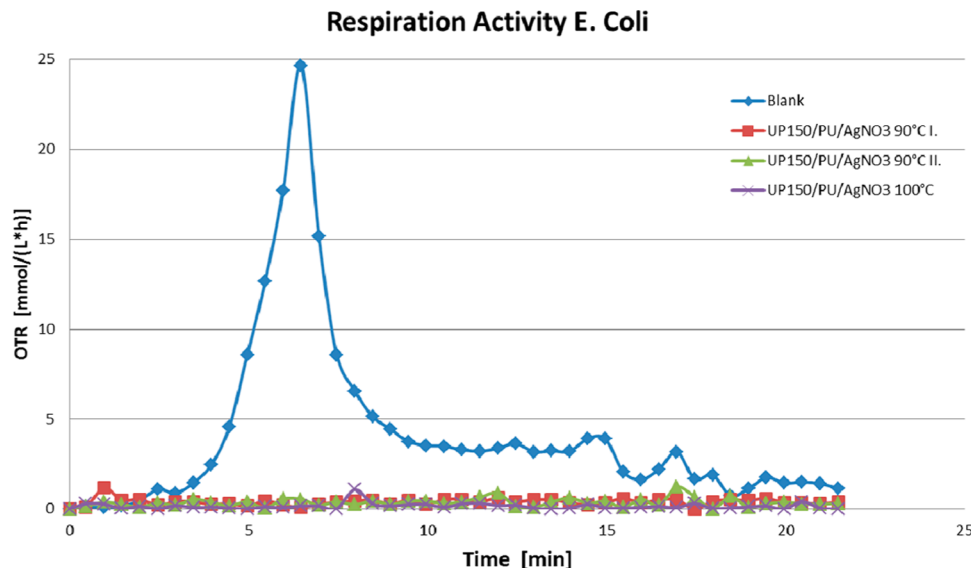


Figure 9. Oxygen transfer rate of *E. coli*, using three different silver-coated membranes.

provided by Institute of Macromolecular Chemistry revealed that the silver particles are positioned mainly on the nanofiber surface.

3.2. PES Nanofibers. We tested a range of solvents as electrospinning solutions, each of which produced functional samples with different fiber formations (Figure 3). The best results were achieved using highly soluble silver nitrate with silver benzoate as the organic silver carboxylate precursor.

Both silver nitrate and silver benzoate resulted in particles smaller than the fiber diameter (Table 1). This was confirmed by both SEM images and from the complementary color spectrum of visible light. In general, when electrospinning creates fine fibers, particles are also small and homogeneous. The optimal silver concentration was obtained by undertaking a set of experiments with a range of silver concentrations and with process parameters close to those without any addition of silver.

A NEP/silver behenate dispersal was preferable as PES is more soluble in NEP than PU.⁷ In laboratory experiments, however, mass flow from the spinning drop between the electrodes was not homogeneous and the total silver amount, together with fine fiber delivery, was suboptimal, even with a wide voltage range (20–50 kV).

In the case of NEP/silver behenate dispersal, the particle size was smaller than the fiber diameter (~ 100 nm) with a higher homogeneity compared to PU. Because of their hygroscopic properties, however, water-based silver dispersal solutions were not successfully electrospun.

Mean particle size in the silver nitrate (DMF/DMAc) solution was 90 nm (14% wt_P), and ~ 40 nm (8.0% wt_P) in the silver benzoate (DMF/DMAc). Using the silver behenate precursor (DMF/NMP with DMSO as additive), particle sizes of ~ 200 nm were achieved, without homogeneous delivery.

3.3. Fibers Cast by Continuous Electrospinning. A basic PU solution with silver nitrate, and PES solutions with silver nitrate, silver benzoate, and silver behenate dispersion, were continuously spun successfully and tested further (see Table 2).

Fibers from PU with reduced silver nitrate (Figure 4) were obtained under the following process conditions: voltage = 68–72 kV, electrode distance = 0.16 m, relative humidity (RH) =

18%–22%, roller speed = 0.05 m/min, and temperature = 26.0–28.0 °C.

3.4. Preparation of Composite Membranes. Thermal Pressure Lamination. Initial experiments on flat sheet membranes indicated that adhesion between nanofibers and the membrane was achievable. However, increased adhesion through thermal pressure lamination led to nanofiber and/or membrane degradation. In the case of PU nanofibers with silver nitrate, structural loss was observed in the nanofiber layer at temperatures above 120 °C; however, PES nanofibers remained stable, even at higher temperatures.

For samples of PU nanofiber with silver nitrate, and for PES nanofiber with silver nitrate, silver benzoate, and silver behenate dispersion, the nanofiber layer was separated from the PP support layer shortly before the lamination step. (See Figure 5). Using the OSHIMA Mini Press, the best results for PES (independent of silver type) were obtained over a temperature range of 135–145 °C and at pressures of 1.6–2.4 kPa, and the best results for PU were obtained at temperatures of 95–100 °C and at a pressure of 2.0 kPa. These modified composite membranes were tested further for permeability and antimicrobial properties.

Nanofiber Deposition Directly on the Membrane Surface. SEM imaging confirmed that directly cast nanofiber layers were uniformly deposited (Figure 6). However, the limiting factor during this procedure is likely to be residual solvent content. While permeability declined using this procedure; the process resulted in a lower drop in permeability than when using thermal pressure lamination.

Reduction Methods for Silver Nanoparticles. The reduction method of silver in DMF was proven to be efficient for silver solvent reduction. This step is recommended before the polymer addition to solvent-reduction system. The ex-post-reduction conducted by diluted ascorbic acid leads to perceptible morphology changes of nanofiber structure. The UVA ex-post-reduction proved the most effective method, in terms of lowest chemical influence on nanofiber morphology and color change efficiency.

3.5. Membrane Testing. Membrane Permeability. Both testing protocols confirmed that increased lamination temperature decreased permeability for both empty membranes and

composite nanofiber membranes, with the latter being more significant. PES nanofibers exhibited excellent dimensional stability; however, only high lamination temperatures ensured good adhesion to the supporting membrane, which resulted in deterioration in the supporting membrane pore structure.

As both membrane and nanofibers suffered at high temperatures, two future concepts were assessed: (a) the use of different polymers with good adhesion to PES membranes at lower temperatures, and/or (b) elimination of the lamination process completely.

PU nanofibers, which require lower temperatures for good adhesion, provide greater permeability. Permeability values were still lower than those of empty membranes; therefore, a composite membrane without lamination was developed. Figure 7 shows the development of composite membrane permeability achieved without thermal pressure lamination. Typically, empty membranes had twice the permeability of laminated membranes. Casting PU nanofibers directly onto the membrane's surface, rather than through lamination, improved permeability by ~50%.

As shown in Figure 7, nanofiber layers added by thermal pressure lamination showed increased resistance, compared to free deposition. Because of the very high porosity of nanofiber layers with a fiber diameter in the 200-nm range, resistance is expected to be orders of magnitude lower than that for 150 kDa ultrafiltration membranes. The increase in resistance can be explained by residual solvent flow, which could block some of the membrane pores and could transform some nanofibers into less-porous interconnected structures.

If transport is mainly determined by electrochemical potential, then both the pure water and wastewater transport mechanism could be affected by internal polarization. We assume that the nanofiber's porous structure provides water transport sufficient to quickly equal any electrochemical differences, such that transport is mainly determined by pressure difference. In cases where the transport layer is, e.g., membranes for nanofiltration or reverse osmosis, the influence of internal polarization could be more significant¹⁸ and could lower the desired transport.¹⁹ Composite membrane permeability will never be as high as that of empty membranes; however, this is the price paid for the added antibacterial functionality.

Leaching of Silver from the Nanofiber Layer. Our experiments indicate that silver is passed through a 150 kDa MWCO membrane, even though this is denser than the reported particle sizes listed in Table 1. This is due to the silver dissolving and Ag⁺ ions passing through the membrane, not the particles themselves.

Excessive leaching of silver antibacterial particles from the nanofiber layer into wastewater is potentially a serious environmental problem and a recognized drawback of present methodology. Furthermore, excessive silver leaching reduces the long-term biocidal properties of the nanofiber layer. For these reasons, we focused on the leaching characteristics of the nanofiber layer with the best antibacterial properties, i.e., PU nanofibers with silver nitrate on Nadir UP150. A very similar leaching pattern was observed, independent of the initial silver content (typically 800 mg/m²) (Figure 8a). Most of the silver was washed out in the first permeating milliliters, and was directly proportional to the initial amount of silver in the nanofiber layer. There was no difference in leaching between laminated and free deposition membranes. When left mixing in DEMI water, the concentration of silver stopped increasing

after 1 h and remained constant at the expected amount (i.e. 800 mg/m²), which corresponds to the amount of silver added during electrospinning (see Figure 8b).

The same experiment, extended to four days, showed that silver leaching stopped after ~1 h and from then on the concentration of silver remained constant. There was no significant difference between the integration and derivation methods, meaning that leaching did not stop due to concentration equilibrium on the nanofiber's surface and in water, but that the remaining silver was actually fixed on the nanofiber's surface, providing positive antibacterial activity (see biocide tests for 4-day leaching).

SEM scans indicated excess silver in the dry samples: with small silver particles visible on the fiber surfaces after 1 min (Figure 8a), and aggregation of silver after 10 min (Figure 8b).

Antibacterial Properties: CFU. Several nanofiber and silver combinations were tested (i.e., PU + silver nitrate, PES + silver nitrate, PES + silver benzoate, PES + silver behenate) using both deposition methods, with the best antibacterial properties being obtained using a continuous electrospinning of PU nanofibers with silver nitrate.

Because of significant silver leaching in the permeating liquid, the question of long-term stability of nanofiber antibacterial properties remains open. In order to verify antibacterial stability over time, the leaching tests were carried out using 20 times higher permeate volume and approximately twice the bacterial content (300 CFU to 336 cm² of membrane in Alfa Laval M10, as opposed to 5 CFU per 13.4 cm² using a dead-end Amicon cell). No bacterial growth was observed on the membrane using this arrangement.

The midterm biocide test of the count formation units per milliliter, as shown in Table 3, proved the biocide effect of modified membranes after 4 days of leaching.

Antibacterial Properties: Respiration Activity. Three different silver-coated membranes (Nadir UP150) were tested against a blank sample (samples I and II used the same lamination conditions and were used for reproducibility). Very strong antibacterial properties were illustrated for all three membranes (Figure 9).

4. CONCLUSIONS

It is possible to combine colloidal zero-valent, organic, and inorganic silver with nanofiber structures, with the best results obtained for highly soluble silver nitrate and silver benzoate, rather than silver behenate. However, this latter form is still an interesting alternative, because it promises better stability for long-term applications.

There are two possible methods for preparing composite ultrafiltration membranes with antibacterial properties: (a) direct nanofiber deposition and (b) thermal pressure lamination. However, added functionality comes at the expense of lower permeability, which can be improved by optimizing the deposition process.

Biocidal properties over both short- and long-term operation were confirmed using two different methods (CFU and respiratory), while concurrently monitoring how added silver leached from the nanofiber layer.

Future research will be based on (a) optimizing the silver content in nanofibers, (b) optimizing the nanofiber diameter in order to minimize leaching, and (c) testing the membranes under actual ultrafiltration conditions and using actual wastewater.

AUTHOR INFORMATION

Corresponding Author

*E-mail: jan.dolina@tul.cz.

Author Contributions

All authors contributed equally to the manuscript and all authors have given approval to the final version of the manuscript.

Notes

The authors declare no competing financial interest.

ACKNOWLEDGMENTS

The work of J.D. and T.J. was supported by the Ministry of Education of the Czech Republic within the Project No. 78001 of the Technical University of Liberec. The research reported in this paper was supported in part by the projects NAMETECH (GA No. 226791), part of the European Commission's 7th Framework Programme and OP VaVpI Centre for Nanomaterials, Advanced Technologies and Innovation (No. CZ.1.05/2.1.00/01.0005). The authors wish to thank project sources, as well as the TUL department of nonwoven textiles for technical and material support.

REFERENCES

- (1) Dvořák, L.; Gómez, M.; Dvořáková, M.; Růžičková, I.; Wanner, J. The impact of different operating conditions on membrane fouling and EPS production. *Bioresour. Technol.* **2011**, *102*, 6870–6875.
- (2) Genné, I.; Doyen, W.; Kupers, S.; Leysen, R. Formation and characteristics of organo-mineral membranes. *Proc. Euromembrane* **1995**, *1*, 245–249.
- (3) Kochan, J.; Wintgens, T.; Wong, J. E.; Melin, T. Properties of polyethersulfone ultrafiltration membranes modified by polyelectrolytes. *Desalination* **2010**, *250*, 1008–1010.
- (4) Morones, J. R.; Elechiguerra, J. L.; Camacho, A.; Holt, K.; Kouri, J. B.; Ramírez, J. T.; Yacaman, M. J. The bacterial effect of silver nanoparticles. *Nanotechnology* **2005**, *16*, 2346.
- (5) Huang, Z. M.; Zhang, Y. Z.; Kotaki, M.; Ramakrishna, S. A review on polymer nanofibers by electrospinning and their applications in nanocomposites. *Compos. Sci. Technol.* **2003**, *63*, 2223–2253.
- (6) Seymour, R. B.; Kauffman, G. B. Polyurethanes: A Class of Modern Versatile Materials. *J. Chem. Educ.* **1992**, *69*, 909.
- (7) Hansen, Ch. M. *Hansen Solubility Parameters: A User's Handbook*; CRC Press: Boca Raton, FL, 2007.
- (8) Jirsák, O.; Sanetrník, F.; Lukáš, D.; Kotek, V.; Martinová, L.; Chaloupek, J. *A Method of nanofiber production from polymer solution using electrostatic spinning and a device for carrying out the method*. U.S. Patent 7,585,437, 2009.
- (9) Panacek, A.; Kvítek, L.; Prucek, R.; Kolar, M.; Vecerova, R.; Pizúrova, N.; Sharma, V. K.; Nevecna, T.; Zboril, R. Silver colloid nanoparticles: synthesis, characterization, and their antibacterial activity. *J. Phys. Chem.* **2006**, *24*, 16248–53.
- (10) Santos, I. P.; Marzán, L. M. Reduction of silver nanoparticles in DMF. Formation of monolayers and stable colloids. *Pure Appl. Chem.* **2000**, *72*, 83–90.
- (11) Chou, K. S.; Lu, Y. Ch.; Lee, H. H. Effect of alkaline ion on the mechanism and kinetics of chemical reduction of silver. *Mater. Chem. Phys.* **2005**, *94*, 429–433.
- (12) Chadal, R. P.; Mahendia, S.; Tomar, A. K. Effect of ultraviolet irradiation on the optical and structural characteristics of in-situ prepared PVP-Ag nanocomposites. *Digest J. Nanomater. Biostruct.* **2011**, *6*, 299–306.
- (13) Haberkamp, J.; Ernst, M.; Makdissi, G.; Huck, P. M.; Jekel, M. Protein Fouling of Ultrafiltration Membranes—Investigation of Several Factors Relevant for Tertiary Wastewater Treatment. *J. Environ. Eng. Sci.* **2008**, *7*, 1–3.
- (14) Tang, Z.; Qiu, Ch.; McCutcheon, J. R.; Yoon, K.; Ma, H.; Fang, D.; Lee, E.; Kopp, C.; Hsiao, B. S.; Chu, B. Design and Fabrication of Electrospun PES Nanofibrous Scaffold. *J. Polym. Sci.* **2009**, *47*, 2288–2300.
- (15) Anderlei, T.; Zang, W.; Papaspyrou, M.; Buchs, J. Online respiration activity measurement (OTR, CTR, RQ) in shake flasks. *Biochem. Eng. J.* **2004**, *17*, 187–194.
- (16) Phillips, R.; Kondev, J.; Theriot, J. *Physical Biology of the Cell*; Garland Science: London, 2008.
- (17) Miller, J. K.; Neubig, R.; Clemons, C. B.; Kreider, K. L.; Wilber, J. P.; Young, G. W.; Ditto, A. J.; Yun, Y. H.; Milsted, A.; Badawy, H. T.; Panzner, M. J.; Youngs, W. J.; Cannon, C. L. Nanoparticle deposition onto biofilms. *Biomed. Eng.* **2013**, *41*, 53–67.
- (18) Cath, T. Y.; Childress, A. B.; Elimelech, M. Forward osmosis: Principles, applications, and recent developments. *J. Membr. Sci.* **2006**, *281*, 70–87.
- (19) Mulder, M. *Basic Principles of Membrane Technology*; Kluwer Academic Publishers: Dordrecht, The Netherlands, 1996.